Mode Switching for SWIPT Over Fading Channel With Nonlinear Energy Harvesting

Jae-Mo Kang, Il-Min Kim, *Senior Member, IEEE*, and Dong In Kim, *Senior Member, IEEE*

***Abstract*—We study mode switching (MS) between information decoding and energy harvesting (EH) for simultaneous wireless information and power transfer (SWIPT) over the fading channel. Unlike the existing result obtained with a simplistic assumption of linear EH, we consider a realistic scenario of the nonlinear EH. In this setting, to design the optimal MS, we address the problem of maximizing the average achievable rate under an average harvested energy constraint, which is generally nonconvex and combinatorial. Using the time-sharing condition, the optimal MS solution for the nonlinear EH is presented efficiently. From the obtained result and further analysis, we draw interesting and important insights into the optimized SWIPT system with nonlinear EH.**

***Index Terms*—Fading channel, mode switching, nonlinear energy harvesting, SWIPT.**

I. Introduction

SIMULTANEOUS wireless information and power transfer (SWIPT) using radio frequency (RF) waves has recently drawn an upsurge of research interest in the literature. In [1] and [2], several practical SWIPT schemes were proposed considering the limitation of the currently adopted circuits that both information decoding (ID) and energy harvesting (EH) cannot be carried out at the same time using the same received signal.[1] Based on these schemes, in [1]–[3], the ultimate performance limits of various SWIPT systems were studied focusing on the additive Gaussian channels without fading.

For the SWIPT system over the fading channel, the mode switching (MS) scheme was studied in [5], which dynamically switches between the ID and EH modes at each fading state. In [5], however, the ideal and simplistic linear EH model was assumed, in which the harvested energy always increases linearly with the received power given a constant EH efficiency (or energy conversion efficiency). However, it is not practical to simply assume that the EH circuit operates linearly because there are various sources of nonlinearity, e.g., the diodes, inductors, and capacitors used in the rectifier, which are all nonlinear devices [6]–[14]. Furthermore, the experimental results clearly show that the practical EH circuits are highly nonlinear [6]–[8]. This is because the EH efficiency becomes different (not constant) depending on the received power level. Specifically, as validated by the field measurements in [6]–[8] (or see [14, Fig. 2]) and pointed out in [9] and [14], the EH efficiency of the actual EH circuit is (very) small when the received power is (very) low due to the diode turn-on voltage and it initially increases when the received power increases to a certain level. But, when the received power exceeds a certain level, the EH efficiency is degraded and the amount of harvested energy eventually saturates due to the reverse breakdown of the diode [6], [8], [9], [14]. Due to such nonlinearity issue, the previous result of [5] obtained with the ideal linear EH model might lead to misleading or wrong conclusion for the practical nonlinear EH circuits. To the best of our knowledge, this issue has not been addressed nor resolved in the literature. This motivated our work.

In this letter, we investigate the MS scheme for the SWIPT over the fading channel considering the nonlinear EH. We adopt a realistic nonlinear EH model suggested in [14], which was shown to accurately match the experimental results reported in [7] and [8]. For the adopted nonlinear EH model, the MS problem is in general nonconvex and combinatorial, and thus, it is challenging to solve. To overcome the difficulty, we exploit the time-sharing property and solve the MS problem efficiently. Overall, the contributions of this letter are as follows. First, we derive the optimal MS solution for the nonlinear EH. Second, the MS results for the nonlinear EH and linear EH are compared, and their MS regions are analyzed. Particularly, we draw interesting insights into the practical nonlinear EH: the EH mode is selected only for the moderate channel gains, and the ID mode is selected for low or high channel gains, which are in sharp contrast to the ideal case of linear EH.

II. System Model and Problem Formulation

A. System Model

We consider a point-to-point SWIPT system with one transmitter and one receiver, each equipped with a single antenna. We assume the block fading model, i.e., the channel remains constant during the period of one fading block, but it varies block to block independently. Over the fading blocks, the transmitter sends a codeword, which is composed of independent Gaussian distributed symbols with power P. Let h denote the power gain of the fading channel, which is assumed to be ergodic.

We adopt the MS scheme at the receiver, which can be easily implemented via the low-complexity time switcher. At each fading state, the receiver can operate either in the ID or EH mode. We define the *binary* variable $\alpha \in \{0, 1\}$ to indicate

Manuscript received July 4, 2017; revised July 13, 2017; accepted July 15, 2017. Date of publication July 20, 2017; date of current version October 11, 2017. This work was supported in part by the Natural Sciences and Engineering Research Council of Canada, and in part by the National Research Foundation of Korea Grant funded by the Korean Government under Grant 2014R1A5A1011478. The associate editor coordinating the review of this paper and approving it for publication was J. Xu. *(Corresponding author: Dong In Kim.)*

J.-M. Kang and I.-M. Kim are with the Department of Electrical and Computer Engineering, Queen's University, Kingston, ON K7L 3N6, Canada (e-mail: jaemo.kang@queensu.ca; ilmin.kim@queensu.ca).

D. I. Kim is with the School of Information and Communication Engineering, Sungkyunkwan University, Suwon 440-746, South Korea (e-mail: dikim@skku.ac.kr).

Digital Object Identifier 10.1109/LWC.2017.2729554

[1] Actually, based on the results in thermodynamics of computing, it is possible to demonstrate that the energy may not need to be dissipated in the decoding process [4, Ch. 5].

2162-2345 © 2017 IEEE. Personal use is permitted, but republication/redistribution requires IEEE permission.
See http://www.ieee.org/publications_standards/publications/rights/index.html for more information.

Authorized licensed use limited to: Sungkyunkwan University. Downloaded on March 08,2023 at 11:31:22 UTC from IEEE Xplore. Restrictions apply.

the operation mode as follows:

$$\alpha = \begin{cases} 0, & \text{if the selected mode is ID} \\ 1, & \text{if the selected mode is EH.} \end{cases} \quad (1)$$

With the MS, it is easy to see that the average achievable rate is given by $\mathbb{E}[R(\alpha)]$, where

$$R(\alpha) = (1-\alpha)\log_2\left(1+\frac{hP}{\sigma^2}\right) \quad (2)$$

and σ^2 is the variance of the additive Gaussian noise. Also, the expectation is taken over the random channel gain h.

B. Nonlinear EH Model

We now formulate the amount of harvested energy. In the most existing literature on the SWIPT including [5], the simplistic linear EH model was used, in which the average harvested energy is given by $\mathbb{E}[Q^{\mathrm{L}}(\alpha)]$, where

$$Q^{\mathrm{L}}(\alpha) = \alpha\zeta hP. \quad (3)$$

In (3), $0 < \zeta \leq 1$ is the EH efficiency (or the energy conversion efficiency), which is assumed to be a constant over the entire range of the received power hP. However, the linear EH model of (3) is too ideal, because the practical EH circuit exhibits a nonlinear behavior, mainly due to the diode(s) used in the rectifier circuit [6]–[14]. Specifically, the harvested energy of the EH circuit is proportional to the square of the output direct current (DC) of the diode (or the output DC power of the rectifier), which is highly nonlinear due to the nonlinearity of the diode characteristic equation [2], [11], [12].

To address the nonlinearity issue in the EH, in the literature, various nonlinear EH models were presented [9]–[14]. On one hand, in [9], a nonlinear EH model for a single diode rectifier was suggested based on the circuit analysis. In this nonlinear model, the average harvested energy is expressed as $\mathbb{E}[\widetilde{Q}^{\mathrm{NL}}(\alpha)]$, where $\widetilde{Q}^{\mathrm{NL}}(\alpha) = \alpha\frac{\overline{V}_o^2}{R_l}$. Also, $\overline{V}_o$ denotes the DC component of the output voltage of the rectifier, and R_l the load resistance, which is assumed to be given. At each fading state, the value of $\overline{V}_o$ can be determined by solving the following nonlinear system of equation [9]:

$$e^{\frac{\overline{V}_o}{\eta V_t}}\left(1+\frac{\overline{V}_o}{R_l I_s}\right) = \frac{1}{T}\int_T e^{\frac{\sqrt{R_a}y(t)}{\eta V_t}}dt \quad (4)$$

where η, V_t, and I_s denote the ideality factor, the thermal voltage, and the reverse bias current of the diode, respectively. Also, T, R_a, and $y(t)$ denote the symbol period, the antenna resistance, and the received RF signal, respectively. Using the Taylor series expansion, the integration term $e^{\frac{\sqrt{R_a}y(t)}{\eta V_t}}$ in the right side of (4) can be expressed as $e^{\frac{\sqrt{R_a}y(t)}{\eta V_t}} = \sum_{j=0}^{J}\frac{c_j}{j!}y^j(t)$ with $J \to \infty$, where $c_j = \frac{\sqrt{R_a}}{\eta V_t}$. When $J = 2$ and $J = 4$, respectively, (i.e., the second- and fourth-order truncations), the nonlinear model of [9] corresponds to the linear model and the nonlinear model considered in [10]–[13]. On the other hand, in [14], another nonlinear EH model was suggested based on the logistic function, i.e., S-shape curve. In [14], it was demonstrated that the suggested nonlinear model accurately matches the experimental results such as reported in [7] and [8]. Note that the various nonlinear models of [9]–[14] are all valid if the received power level is less than the diode breakdown threshold. In this letter, we adopt the nonlinear EH model used in [14].[2] In this nonlinear model, the average harvested energy is given by $\mathbb{E}[Q^{\mathrm{NL}}(\alpha)]$, where

$$Q^{\mathrm{NL}}(\alpha) = \alpha\frac{P_s(1-e^{-ahP})}{1+e^{-a(hP-b)}}. \quad (5)$$

In (5), P_s is the maximum harvested power when the EH circuit is saturated. Also, a and b are constants related to the EH circuit specification. Given the EH circuit, one can readily determine P_s, a, and b by the curve fitting method.[3]

C. Problem Formulation

In this letter, using the nonlinear EH model, we consider the average achievable rate maximization problem for the MS under an average harvested energy constraint as follows:

$$\text{(P1)}: \max_{\alpha\in\{0,1\}} \quad \mathbb{E}[R(\alpha)] \quad \mathtt{s.t.} \quad \mathbb{E}[Q^{\mathrm{NL}}(\alpha)] \geq Q.$$

In general, it is difficult to directly solve (P1) since it is a nonconvex combinatorial problem due to the binary variable α, and both the objective and constraint functions involve the expectation over the random variable h. Also, the computational complexity to solve (P1) is generally high since it increases exponentially with the number of blocks. Furthermore, since the linear EH model of (3) and the nonlinear EH model of (5) are mathematically and practically different, the solution given in [5, eq. (34)] might be no longer optimal for the nonlinear EH.

III. Mode Switching for Nonlinear Energy Harvesting

A. Optimal Solution to (P1)

In this subsection, we exploit the so-called time-sharing condition given in [15] to optimally and efficiently solve the challenging problem (P1). Taking the time-sharing between any two optimal solutions to (P1) and using the law of large number, it can be shown that, for the problem (P1), the time-sharing condition in [15, Definition 1] holds.

As shown in [15, Th. 1], if a (nonconvex) problem satisfies the time-sharing condition, then the strong duality always holds, implying zero duality gap. Therefore, the Lagrange duality method can be used to solve the MS problem (P1).[4] Taking this approach, in the following, we present the optimal MS solution for the nonlinear EH.

[2]There are two major differences between the nonlinear model of [14] adopted in our work and those of [9]–[13]. First, the nonlinear models of [10]–[13] are based on the analysis of the diode current, whereas that of [14] is based on the curve fitting of the real measurement data. Second, the nonlinear model of [14] explicitly considers the saturation of the harvested energy, whereas it is not explicitly considered in the nonlinear models of [10]–[13].

[3]Since the parameters P_s, a, and b depend only on the specification of the EH circuit such as the turn-on voltage of the diode and the maximum output DC power of the rectifier [14], they need to be calculated only once given the EH circuit. Thus, even when the transmit signal adaptively varies, those parameters do not need to be adaptively updated.

[4]If α is not restricted to be binary, i.e., $0 \leq \alpha \leq 1$, the (reduced) Lagrange dual function for each fading state is given by $\mathcal{L} = R(\alpha(h)) + \lambda^{\mathrm{NL}}Q^{\mathrm{NL}}(\alpha(h)) + \mu(h)\alpha(h) - \nu(h)(\alpha(h)-1)$. In this case, the solution to (P1) is given by $0 < \alpha^{\mathrm{NL}}(h) < 1$ for one particular fading state and $\alpha^{\mathrm{NL}}(h) \in \{0,1\}$ for the other fading states, since the KKT conditions are given by 1) $r(h) \geq \lambda^{\mathrm{NL}}q^{\mathrm{NL}}(h)$ if $\alpha^{\mathrm{NL}}(h) = 0$ due to $\mu(h) \geq 0$ and $\nu(h) = 0$; 2) $r(h) \leq \lambda^{\mathrm{NL}}q^{\mathrm{NL}}(h)$ if $\alpha^{\mathrm{NL}}(h) = 1$ due to $\mu(h) = 0$ and $\nu(h) \geq 0$; and 3) $r(h) = \lambda^{\mathrm{NL}}q^{\mathrm{NL}}(h)$ if $0 < \alpha^{\mathrm{NL}}(h) < 1$ due to $\mu(h) = \nu(h) = 0$.

Authorized licensed use limited to: Sungkyunkwan University. Downloaded on March 08,2023 at 11:31:22 UTC from IEEE Xplore. Restrictions apply.

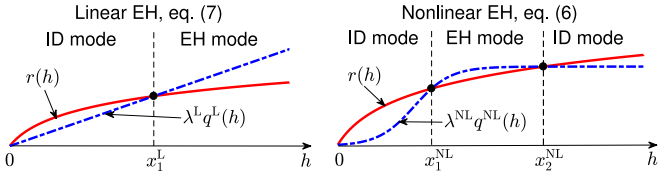

Fig. 1. Comparison of MS results for the linear EH and nonlinear EH.

Lemma 1: The optimal solution to (P1) is given by

$$\alpha^{\mathrm{NL}}(h) = \begin{cases} 0, & \text{if } h < x_1^{\mathrm{NL}} \text{ or } h > x_2^{\mathrm{NL}} \\ 1, & \text{if } x_1^{\mathrm{NL}} \le h \le x_2^{\mathrm{NL}} \end{cases}. \tag{6}$$

In (6), x_1^{NL} and x_2^{NL} ($> x_1^{\mathrm{NL}}$) are two positive real roots of the equation $r(x) - \lambda^{\mathrm{NL}} q^{\mathrm{NL}}(x) = 0$ over $x \in (0, \infty)$, where $r(x) = \log_2\left(1 + \frac{xP}{\sigma^2}\right)$ and $q^{\mathrm{NL}}(x) = \frac{P_s(1-e^{-axP})}{1+e^{-a(xP-b)}}$. The constant $\lambda^{\mathrm{NL}} > 0$ is determined such that $\mathbb{E}[Q^{\mathrm{NL}}(\alpha^{\mathrm{NL}}(h))] = Q$.

Proof: See Appendix A. ∎

From Lemma 1, one can see that the computational complexity to solve (P2) can be significantly reduced. Specifically, in (6), we only need to compare the channel power gain to the two thresholds x_1^{NL} and x_2^{NL} at each fading state. Thus, the complexity is now linear in the block-length, not exponential.

In [5, eq. (34)], the optimal MS scheme for the linear EH model $Q^{\mathrm{L}}(\alpha)$ was derived as

$$\alpha^{\mathrm{L}}(h) = \begin{cases} 0, & \text{if } h < x_1^{\mathrm{L}} \\ 1, & \text{if } h \ge x_1^{\mathrm{L}}. \end{cases} \tag{7}$$

In (7), x_1^{L} is the positive root of the equation $r(x) - \lambda^{\mathrm{L}} q^{\mathrm{L}}(x) = 0$ over $x \in (0, \infty)$, where $q^{\mathrm{L}}(x) = \zeta xP$ and the constant $\lambda^{\mathrm{L}} > 0$ is determined such that $\mathbb{E}[Q^{\mathrm{L}}(\alpha^{\mathrm{L}}(h))] = Q$.

In order to draw interesting insights, in the following subsections, the MS results of (6) and (7) are compared and their MS regions are analyzed.

B. Comparison of Mode Switching Results for Nonlinear EH and Linear EH

In Fig. 1, for comparison, we illustrate the MS result of (7) for the linear EH and that of (6) for the nonlinear EH by analytically plotting the curves of the rate $r(h)$ and the weighted harvested energies $\lambda^{\mathrm{L}} q^{\mathrm{L}}(h)$ and $\lambda^{\mathrm{NL}} q^{\mathrm{NL}}(h)$ over all possible values of the channel power gain h. Note that $r(h)$ is a log function of h. On the other hand, $\lambda^{\mathrm{L}} q(h)^{\mathrm{L}}$ is a linear function of h, whereas $\lambda^{\mathrm{NL}} q(h)^{\mathrm{NL}}$ is a logistic function. For the linear EH, the EH (or ID) mode is selected for the large (or small) channel gain with $h \ge x_1^{\mathrm{L}}$ (or $h < x_1^{\mathrm{L}}$) because the increment of $\lambda^{\mathrm{L}} q(h)^{\mathrm{L}}$ is more (or less) than that of $r(h)$ when $h \ge x_1^{\mathrm{L}}$. However, for the nonlinear EH, the MS strategy becomes quite different. Specifically, the ID mode is selected for the small channel gain with $h < x_1^{\mathrm{NL}}$ or the large channel gain with $h > x_2^{\mathrm{NL}}$, since $r(h) > \lambda^{\mathrm{NL}} q^{\mathrm{NL}}(h)$. On the other hand, the ED mode is selected only for the moderate channel gain with $x_1^{\mathrm{NL}} \le h \le x_2^{\mathrm{NL}}$, since $r(h) < \lambda^{\mathrm{NL}} q^{\mathrm{NL}}(h)$. This very interesting and important result can be intuitively explained as follows: for the nonlinear EH case, only the moderate range of channel gain needs to be used for EH in order to exploit the high EH efficiency in the near-linear region of the EH circuit.

Overall, for the case of linear EH, there are *two* different regions of MS; whereas, for the case of nonlinear EH, there are *three* different regions of MS. Also, for the linear EH, the EH is selected for *large* channel gains; whereas, for the nonlinear EH, the EH is selected for *moderate* channel gains.

C. Analysis of Mode Switching Regions

For analysis, we consider the Rician block fading model; that is, the complex baseband channel is the Gaussian random variable with mean l and variance s, where l accounts for the line of sight (LOS) component and s denotes the average power gain of the scattered component. Thus, the channel power gain h is the non-central chi-squared random variable with the non-centrality parameter $z = |l|^2$. Considering the distance-dependent path loss, the power gains of the LOS and scattered components are modelled as $z = \frac{rc^{-1}d^{-\theta}}{r+1}$ and $s = \frac{c^{-1}d^{-\theta}}{r+1}$, respectively, where d is the distance between the transmitter and the receiver; c a constant related to the reference distance; θ the path loss exponent; and r the Rician factor.

From (6) and after some mathematical manipulations, for the nonlinear EH, the probabilities that the ID and EH modes are selected can be, respectively, calculated as

$$\begin{aligned} P_{\mathrm{ID}}^{\mathrm{NL}} &= \Pr(h < x_1^{\mathrm{NL}}, h > x_2^{\mathrm{NL}}) \\ &= 1 - \mathrm{Q}_1\left(\sqrt{2r}, \sqrt{\gamma x_1^{\mathrm{NL}} d^{\theta}}\right) + \mathrm{Q}_1\left(\sqrt{2r}, \sqrt{\gamma x_2^{\mathrm{NL}} d^{\theta}}\right) \end{aligned} \tag{8}$$

$$\begin{aligned} P_{\mathrm{EH}}^{\mathrm{NL}} &= \Pr(x_1^{\mathrm{NL}} \le h \le x_2^{\mathrm{NL}}) \\ &= \mathrm{Q}_1\left(\sqrt{2r}, \sqrt{\gamma x_1^{\mathrm{NL}} d^{\theta}}\right) - \mathrm{Q}_1\left(\sqrt{2r}, \sqrt{\gamma x_2^{\mathrm{NL}} d^{\theta}}\right) \end{aligned} \tag{9}$$

where $\gamma = c(r+1)^{-1}$; $\mathrm{Q}_m(u, v) = \int_v^{\infty} x\left(\frac{x}{u}\right)^{m-1} e^{-(x^2+u^2)/2} I_{m-1}(ux)dx = e^{-(u^2+v^2)/2} \sum_{n=1-m}^{\infty} \left(\frac{u}{v}\right)^n I_n(uv)$ is the Marcum's Q-function; $I_p(x) = \sum_{n=0}^{\infty} \frac{1}{n!\Gamma(p+n+1)} \left(\frac{x}{2}\right)^{p+2n}$ is the modified Bessel function of the first kind of the pth order; and $\Gamma(x) = \int_0^{\infty} y^{x-1} e^{-y} dy$ is the Gamma function. On the other hand, from (7), the probabilities of the ID and EH modes for the linear EH can be, respectively, calculated as

$$P_{\mathrm{ID}}^{\mathrm{L}} = \Pr(h < x_1^{\mathrm{L}}) = 1 - \mathrm{Q}_1\left(\sqrt{2r}, \sqrt{\gamma x_1^{\mathrm{L}} d^{\theta}}\right) \tag{10}$$

$$P_{\mathrm{EH}}^{\mathrm{L}} = \Pr(h \ge x_1^{\mathrm{L}}) = \mathrm{Q}_1\left(\sqrt{2r}, \sqrt{\gamma x_1^{\mathrm{L}} d^{\theta}}\right). \tag{11}$$

From the results of (8)–(11), we can make the following observations. First, from (10) and (11), it follows that $P_{\mathrm{ID}}^{\mathrm{L}} \to 1$ as $d \to \infty$ and $P_{\mathrm{EH}}^{\mathrm{L}} \to 1$ as $d \to 0$. Thus, for the case of linear EH, the EH (or ID) frequently occurs as the receiver becomes closer to (or farther from) the transmitter, because the channel power gains become larger (or smaller). On the contrary, for the case of nonlinear EH, it follows from (8) and (9) that as $d \to 0$ or $d \to \infty$, we have $P_{\mathrm{ID}}^{\mathrm{L}} \to 1$ and $P_{\mathrm{EH}}^{\mathrm{L}} \to 0$. This means that, as the receiver becomes closer to and farther from the transmitter, the ID mode frequently occurs and the EH mode rarely occurs, because the channel power gains tend to be low and high in those cases. Only at the distances around $d_{\mathrm{EH}}^{\mathrm{NL}} = \arg\max_{d>0}\{P_{\mathrm{EH}}^{\mathrm{NL}}\}$ (corresponding to the moderate channel gains), the EH mode frequently occurs for the case of nonlinear EH.

IV. Numerical Results

In this section, the performance of the proposed MS scheme for the nonlinear EH and the existing MS scheme for the linear EH is numerically compared. The nonlinear EH model of (5) is used for performance evaluation, where we set

Authorized licensed use limited to: Sungkyunkwan University. Downloaded on March 08,2023 at 11:31:22 UTC from IEEE Xplore. Restrictions apply.

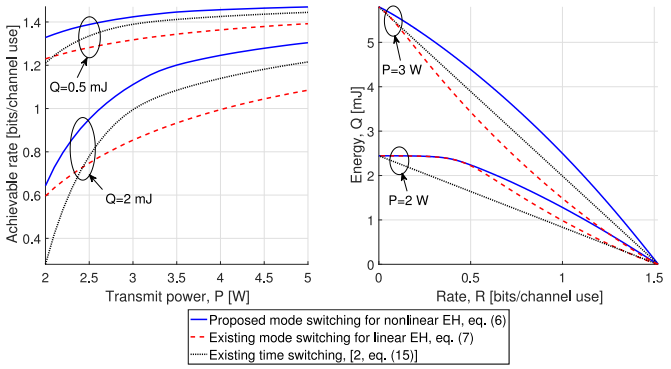

Fig. 2. Achievable rates versus the transmit power P when $Q \in \{0.5, 2\}$ mJ and R-E regions when $P \in \{2, 3\}$ W.

$a = 6400$ and $b = 0.003$, which were obtained in [14] based on the measurement data of [7]. We also present the performance of the TS scheme considered in [2, eq. (15)], which uses a single time switching ratio $0 \le \beta \le 1$ over the fading blocks. In the simulations, we consider $N = 10^5$ fading blocks independently generated from the Rician fading, where the power gains of the LOS and scattered components are set to -30 dB. The noise variance is set such that the average signal to noise ratio is 3 dB. In Fig. 2, the achievable rates are shown versus the transmit power P when $Q \in \{0.5, 2\}$ mJ. Also, the rate-energy (R-E) regions are shown when $P \in \{2, 3\}$ W, where the R-E region is defined as $\mathcal{C}_{\text{R-E}} = \bigcup_{\alpha} \{(R, Q) : Q \le \mathbb{E}[Q^{\text{NL}}(\alpha)], R \le \mathbb{E}[R(\alpha)]\}$, which contains all possible pairs of (R, Q) for the case of nonlinear EH. From Fig. 2, it can be seen that the proposed MS scheme for the nonlinear EH has the best performance in terms of the achievable rate and the R-E tradeoff. When Q is small or P is large, the existing MS scheme for the linear EH is even worse than the existing TS scheme due to the mismatched or inaccurate MS rule.

V. Conclusion

We studied the MS for the SWIPT system over the fading channel considering the nonlinear EH. In this system, we derived the optimal MS solution. The MS results of the nonlinear EH and linear EH were compared, and their MS regions were analyzed, from which the interesting and important insights were drawn.

In this letter, for the realistic nonlinear EH model used in [14], we studied the MS. However, studying the MS scheme for another realistic nonlinear EH models such as considered in [9]–[13] is an important and interesting issue to be investigated as a future work.

Appendix A
Proof of Lemma 1

The Lagrange dual function for (P1) is given by $g(\lambda) = \max_{\alpha \in \{0,1\}} \mathbb{E}[R(\alpha)] + \lambda^{\text{NL}}\big(\mathbb{E}[Q^{\text{NL}}(\alpha)] - Q\big)$, where λ^{NL} is the dual variable associated with the average harvested energy constraint, which can be determined by solving the following dual problem: $\min_{\lambda^{\text{NL}} \ge 0} g(\lambda^{\text{NL}})$. Given the dual variable λ^{NL}, the problem for obtaining the Lagrange dual function can be decomposed into parallel subproblems, each for the particular fading state h, as follows: $\max_{\alpha(h) \in \{0,1\}} R(\alpha(h)) + \lambda^{\text{NL}} Q^{\text{NL}}(\alpha(h))$. To solve this problem, we need to compare the objective values $r(h)$ and $\lambda^{\text{NL}} q^{\text{NL}}(h)$ when $\alpha(h) = 0$ and $\alpha(h) = 1$, respectively, where $r(x) = \log_2\left(1 + \frac{xP}{\sigma^2}\right)$ and $q^{\text{NL}}(x) = \frac{P_s(1 - e^{-axP})}{1 + e^{-a(xP - b)}}$, for $x \in (0, \infty)$. It can be shown that the equation $r(x) = \lambda^{\text{NL}} q^{\text{NL}}(x)$ has two positive real roots x_1^{NL} and x_2^{NL} $(> x_1^{\text{NL}})$, and it follows that $r(x) > \lambda^{\text{NL}} q^{\text{NL}}(x)$ over the intervals $x \in (0, x_1^{\text{NL}})$ and $x \in (x_2^{\text{NL}}, \infty)$. Thus, if $h < x_1^{\text{NL}}$ or $h > x_2^{\text{NL}}$, we have $\alpha^{\text{NL}}(h) = 0$ since $r(h) > \lambda^{\text{NL}} q^{\text{NL}}(h)$. Otherwise, we have $\alpha^{\text{NL}}(h) = 1$ since $r(h) \le \lambda^{\text{NL}} q^{\text{NL}}(h)$. Thus, the solution can be expressed as in (6). To find the optimal dual variable λ^{NL}, the following completeness slackness condition must be satisfied: $\lambda^{\text{NL}}\big(\mathbb{E}[Q^{\text{NL}}(\alpha^{\text{NL}}(h))] - Q\big) = 0$. Without loss of generality, we assume that $Q > 0$. If $\lambda^{\text{NL}} = 0$, we have $\alpha^{\text{NL}}(h) = 0$ for all the fading states, which is infeasible for (P1). Thus, it should be $\lambda^{\text{NL}} > 0$. To satisfy the completeness slackness condition, λ^{NL} should be chosen such that $\mathbb{E}[Q^{\text{NL}}(\alpha^{\text{NL}}(h))] = Q$.

References

[1] R. Zhang and C. K. Ho, "MIMO broadcasting for simultaneous wireless information and power transfer," *IEEE Trans. Wireless Commun.*, vol. 12, no. 5, pp. 1989–2001, May 2013.

[2] X. Zhou, R. Zhang, and C. K. Ho, "Wireless information and power transfer: Architecture design and rate-energy tradeoff," *IEEE Trans. Commun.*, vol. 61, no. 11, pp. 4753–4767, Nov. 2013.

[3] I.-M. Kim and D. I. Kim, "Wireless information and power transfer: Rate-energy tradeoff for equi-probable arbitrary-shaped discrete inputs," *IEEE Trans. Wireless Commun.*, vol. 15, no. 6, pp. 4393–4407, Jun. 2016.

[4] R. P. Feynman, *Feynman Lectures on Computation*, J. G. Hey and R. W. Allen, Eds. Boston, MA, USA: Addison-Wesley, 1998.

[5] L. Liu, R. Zhang, and K.-C. Chua, "Wireless information transfer with opportunistic energy harvesting," *IEEE Trans. Wireless Commun.*, vol. 12, no. 1, pp. 288–300, Jan. 2013.

[6] C. R. Valenta and G. D. Durgin, "Harvesting wireless power: Survey of energy-harvester conversion efficiency in far-field, wireless power transfer systems," *IEEE Microw. Mag.*, vol. 15, no. 4, pp. 108–120, Jun. 2014.

[7] T. Le, K. Mayaram, and T. Fiez, "Efficient far-field radio frequency energy harvesting for passively powered sensor networks," *IEEE J. Solid-State Circuits*, vol. 43, no. 5, pp. 1287–1302, May 2008.

[8] J. Guo and X. Zhu, "An improved analytical model for RF-DC conversion efficiency in microwave rectifiers," in *Proc. IEEE MTT-S Int. Microw. Symp. Dig.*, Montreal, QC, Canada, 2012, pp. 1–3.

[9] M. R. V. Moghadam, Y. Zeng, and R. Zhang. (2017). *Waveform Optimization for Radio-Frequency Wireless Power Transfer*. [Online]. Available: https://arxiv.org/abs/1703.04006

[10] D. I. Kim, J. H. Moon, and J. J. Park, "New SWIPT using PAPR: How it works," *IEEE Wireless Commun. Lett.*, vol. 5, no. 6, pp. 672–675, Dec. 2016.

[11] Y. Zeng, B. Clerckx, and R. Zhang, "Communications and signals design for wireless power transmission," *IEEE Trans. Commun.*, vol. 65, no. 5, pp. 2264–2290, May 2017.

[12] B. Clerckx and E. Bayguzina, "Waveform design for wireless power transfer," *IEEE Trans. Signal Process.*, vol. 64, no. 23, pp. 6313–6328, Dec. 2016.

[13] M. Varasteh, B. Rassouli, and B. Clerckx. (2017). *Wireless Information and Power Transfer Over an AWGN Channel: Nonlinearity and Asymmetric Gaussian Signaling*. [Online]. Available: http://arxiv.org/abs/1705.06350

[14] E. Boshkovska, D. W. K. Ng, N. Zlatanov, and R. Schober, "Practical non-linear energy harvesting model and resource allocation for SWIPT systems," *IEEE Commun. Lett.*, vol. 19, no. 12, pp. 2082–2085, Dec. 2015.

[15] W. Yu and R. Lui, "Dual methods for nonconvex spectrum optimization of multicarrier systems," *IEEE Trans. Commun.*, vol. 54, no. 7, pp. 1310–1322, Jul. 2006.

Authorized licensed use limited to: Sungkyunkwan University. Downloaded on March 08,2023 at 11:31:22 UTC from IEEE Xplore. Restrictions apply.